

A New Class of Ferromagnetically-Coupled Mixed Valence Vanadium(IV/V) Polyoxometalates

Manolis J. Manos,^[a] Anastasios J. Tasiopoulos,^[a] Evangelos J. Tolis,^[a] Nicolía Lalioti,^[b] J. Derek Woollins,^[c] Alexandra M. Z. Slawin,^{*[c]} Michael P. Sigalas,^{*[d]} and Themistoklis A. Kabanos^{*[a]}

Abstract: Reaction of $[V^{VI}OCl_2(thf)_2]$ with a bidentate nitrogen-donor ligand (L: phen = 1,10-phenanthroline, 5-mephen = 5-methyl-1,10-phenanthroline, bipy = 2,2'-bipyridine, 5,5'-me₂bipy = 5,5'-dimethyl-2,2'-bipy) in methyl alcohol, in the presence of triethylamine, leads to the formation of hexameric $[V_2^{IV}V_4^V]$ oxo-alkoxo-vanadates of the general formula $[V_6O_{12}(\mu_2-OCH_3)_4(L)_4] \cdot xH_2O$ [L = phen (**1**·4H₂O), 5-mephen (**2**·6H₂O), bipy (**3**·4H₂O), 5,5'-me₂bipy (**4**·H₂O)]. X-ray structure analysis of **1**·2H₂O and **4**·8CH₃OH revealed a pair of V₃O₁₃N₄ trimeric units sharing two corners, with a centrosymmetric planar V₆-core. In addition, a fully oxidized V^V species

$[V^V_4O_8(OCH_3)_2(\mu_3-OCH_3)_2(5,5'-me_2bipy)_2] \cdot 3CH_3OH$ (**5**·3CH₃OH) was isolated from the reaction mixture used for the synthesis of **4**·H₂O. The crystal structure of **5**·3CH₃OH revealed a dicubane-like framework with two missing vertices. Electron paramagnetic resonance (EPR) and variable temperature magnetic susceptibility studies for the hexamers **1**·4H₂O and **3**·4H₂O showed the complete localization of the single 3d electrons on the V^{IV} ions and unusual

ferromagnetic interaction between the two paramagnetic vanadium(IV) ions separated by a distance of about 5.1 Å. Furthermore, intermolecular antiferromagnetic interactions through π -contacts of phenyl rings were observed for these species below 8 K. The ferromagnetic exchange coupling observed in the hexanuclear compounds **1**·4H₂O and **3**·4H₂O is also discussed using ab initio UHF calculations on a model compound. The value of the exchange coupling constant (3.7 cm⁻¹) for this model compound, calculated using the broken symmetry approach, is in good agreement, both in sign and magnitude, with the experimental *J* values (6.00 cm⁻¹ for **1**·4H₂O and 8.54 cm⁻¹ for **3**·4H₂O).

Keywords: ferromagnetism · intermolecular interaction · polyoxometalates · UHF calculations · vanadium

Introduction

Magnetic clusters, that is, molecular assemblies formed by a finite number of exchange-coupled paramagnetic centers,

[a] Dr. T. A. Kabanos, M. J. Manos, Dr. A. J. Tasiopoulos, Dr. E. J. Tolis

Department of Chemistry
Section of Inorganic and Analytical Chemistry
University of Ioannina
45110 Ioannina (Greece)
E-mail: tkampano@cc.uoi.gr

[b] Dr. N. Lalioti

Department of Materials Science
University of Patras
26504 Patras (Greece)
E-mail: vtango@upatras.gr

[c] Dr. A. M. Z. Slawin, Prof. J. D. Woollins

Department of Chemistry
University of St. Andrews
St. Andrews, Fife, KY16 9ST (UK)

[d] Dr. M. P. Sigalas

Department of Chemistry
Laboratory of Applied Quantum Chemistry
Aristotle University of Thessaloniki
54124 Thessaloniki (Greece)
E-mail: sigalas@chem.auth.gr

have received much attention in several areas of research, for example, molecular chemistry, magnetism and biochemistry.^[1] As they lie in between small molecular systems and the bulk state, the limited number of interacting centers often allows us to model their properties with quantum mechanical approaches. They can thus serve as model systems for in-depth understanding of magnetic exchange interactions. On the other hand, when these clusters are large enough, they enter into the realm of nanoscale magnetic materials, which have gained great interest recently and give hope of promising applications.^[2]

A class of inorganic compounds that provide excellent examples of magnetic clusters are the polyoxometalates (POMs). These metal-oxide clusters possess a remarkable degree of molecular and electronic tunabilities that impact in disciplines as diverse as catalysis, medicine and materials science.^[3] However, the importance of polyoxometalates in molecular magnetism is a recent development. Two classes of magnetic POMs have generated significant interest over the last few years. Diamagnetic polyoxo-molybdates or tungstates that encapsulate small clusters of magnetic metal ions, for example, cobalt(II) or nickel(II), constitute one of these

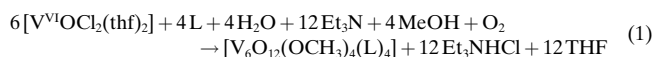
classes.^[4] The second important family of magnetic polyoxometalates comprises the fully reduced V^{IV} and the mixed valence V^{IV/V} oxometalates. The main interest in the mixed valence vanadium(IV/V) clusters arises from the full or partial delocalization of the single 3d electrons of the V^{IV} ions over both V^{IV} and V^V ions, or the complete localization of them on the paramagnetic ions. Magnetic studies performed on polyoxovanadates with 2 to 18 V^{IV} atoms have shown, in most cases, antiferromagnetic coupling between oxovanadium(IV) magnetic ions.^[4] It is noteworthy that the magnetic properties of mixed valence V^{IV/V} oxometalates indicated that the antiferromagnetic coupling is larger than that of their fully reduced V^{IV} analogues, even though a weakening in the vanadium(IV)–vanadium(IV) interactions would be expected due to the increasing number of diamagnetic V^V centers. This stronger antiferromagnetic coupling of the mixed valence V^{IV/V} species has been tentatively attributed to electron-transfer effects.^[4] In general, vanadium is one of the major molecular magnet-forming elements. Vanadium-based magnets with critical temperatures close to room temperature are well known.^[2b, 5] To date, ferromagnetic vanadium compounds are limited to V^{II}^[2b, 5] or V^{III} species.^[6] Examples of ferromagnetically-coupled polynuclear oxovanadium(IV) or (IV/V) systems are very rare.^[7]

We describe herein the synthesis of a series of mixed-valence vanadium(IV/V) polyoxometalates, namely hexanuclear [V₂^{IV}V₄^V] oxo-methoxo-vanadates of the general formula [V₆O₁₂(μ₂-OCH₃)₄(L)₄]_x·xH₂O (where L = a bidentate nitrogen-donor organic ligand such as 1,10-phenanthroline, 2,2'-bipyridine or alkyl-substituted derivatives of these organ-

ic molecules). These compounds were characterized by X-ray crystal structure analysis (**1**·2H₂O, **4**·8CH₃OH), infrared and UV/Vis solid state reflectance spectroscopy as well as elemental and thermogravimetric analyses. The crystal structure and the infrared spectrum of a fully oxidized tetranuclear cluster of the formula [V₄^VO₈(OCH₃)₂(μ₃-OCH₃)₂(5,5'-me₂-bipy)₂]₃·3CH₃OH are also presented. Electron paramagnetic resonance (EPR), variable temperature magnetic susceptibility studies and magnetization measurements for the hexameric species **1**·4H₂O and **3**·4H₂O revealed an unexpected ferromagnetic interaction between two V^{IV} centers separated by a distance of about 5.1 Å and important intermolecular interactions. In addition, ab initio UHF calculations on a simplified model of the hexanuclear clusters have enabled us to obtain both a qualitative interpretation of the ferromagnetic behavior and fairly good quantitative approximations of superexchange coupling constants found experimentally.

Results and Discussion

Synthesis of the compounds: The synthetic procedures to the hexanuclear **1**·4H₂O–**4**·H₂O compounds involve oxidation/hydrolysis reactions of the [V^{IV}OCl₂(thf)₂] precursor in methyl alcohol, in the presence of a nitrogen-donor bidentate ligand and triethylamine. The latter presumably acts as a base, thus facilitating deprotonation of CH₃OH and H₂O molecules [Eq. (1)].

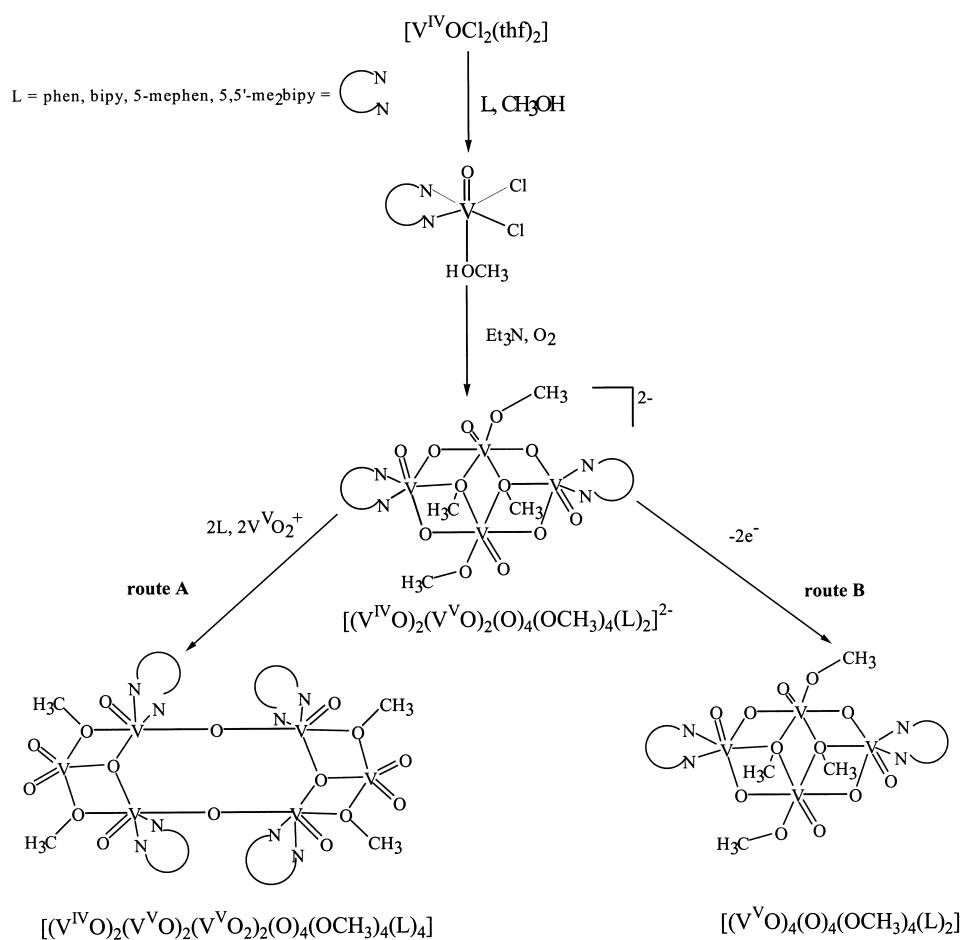


The tetrameric species **5**·3CH₃OH was isolated from the same reaction mixture used for the synthesis of the hexamer **4**·H₂O. Specifically, yellow crystals of **5**·3CH₃OH were precipitated by allowing the solution, from which crystals of **4**·8CH₃OH were also precipitated, to stand at –10 °C for two months. Unfortunately, we have not yet been able to find a reproducible route to the compound **5**·3CH₃OH. Therefore only its crystal structure and infrared spectrum were determined. However, the isolation of **5**·3CH₃OH gave us a clue in our attempt to understand the mechanism of the assembly of the hexanuclear compounds **1**·4H₂O–**4**·H₂O. It is reasonable to assume that the tetranuclear mixed valence V^{IV/V} species, which may result from the fully reduced V₄^{IV} compound, might be an intermediate in the assembly of the hexanuclear compounds **1**·4H₂O–**4**·H₂O (Scheme 1, route A). A small part of this tetranuclear intermediate V^{IV/V} might be fully oxidized, leading to the compound **5**·3CH₃OH (Scheme 1, route B).

X-ray crystallography: X-ray crystal structure analysis of **4**·8CH₃OH (Figure 1) revealed a hexavanadium cyclic system, which has a crystallographic center of symmetry (**1**·2H₂O exhibits a similar gross structure) as well as eight methyl alcohol molecules in the crystal lattice. A selection of interatomic distances and bond angles relevant to the coordination sphere of the vanadium centers for compounds **4**·8CH₃OH and **1**·2H₂O are listed in Table 1. In **4**·8CH₃OH,

Abstract in Greek:

Η αντίδραση του [V^{IV}OCl₂(thf)₂] με ένα διδοντικό υποκαταστάτη L που φέρει άτομα-δότες αζότου (L: phen = 1,10-φαινανθρολίνη, 5-merphen = 5-μέθυλ-1,10-φαινανθρολίνη, bipy = 2,2'-διπυριδίνη, 5,5'-me₂bipy = 5,5'-διμέθυλ-διπυριδίνη) σε μεθανόλη, παρουσία τριαιθυλαμίνης, οδηγεί στο σχηματισμό των εξαμερών [V₂^{IV}V₄^V] οξο-αλκοξο-βαναδικών με το γενικό τύπο [V₆O₁₂(μ₂-OCH₃)₄(L)₄]_xH₂O [L = phen (1·4H₂O), 5-merphen (2·6H₂O), bipy (3·4H₂O), 5,5'-me₂bipy (4·H₂O)]. Η ανάλυση με κρυσταλλογραφία ακτίνων-X των 1·2H₂O και 4·8MeOH αποκάλυψε ένα ζεύγος τριμερών μονάδων V₃O₁₃N₄ που μοιράζονται δύο κορυφές, με μία κεντροσυμμετρική επίπεδη V₆-μονάδα. Επιπλέον, μία πλήρως οξειδωμένη ένωση του V^V [V₄^VO₈(OCH₃)₂(μ₃-OCH₃)₂(5,5'-me₂bipy)₂]₃·3CH₃OH **5**·3CH₃OH, απομονώθηκε από το ίδιο αντιδρών μίγμα με εκείνο που χρησιμοποιήθηκε για την σύνθεση της ένωσης 4·H₂O. Η κρυσταλλική δομή της ένωσης 5·3CH₃OH αποκάλυψε μία δομική μονάδα τύπου-δικουβανίου από το οποίο απουσιάζουν δύο κορυφές. Η φασματοσκοπία ηλεκτρονικού παραμαγνητικού συντονισμού (EPR) και οι μετρήσεις μαγνητικής επιδεκτικότητας σε διάφορες θερμοκρασίες των εξαμερών 1·4H₂O και 3·4H₂O έδειξαν τον πλήρη εντοπισμό των ασύζευκτων 3d ηλεκτρονίων στα ιόντα V^{IV} και μία ασυνήθιστη σιδηρομαγνητική συμπεριφορά μεταξύ δύο παραμαγνητικών ιόντων βαναδίου(IV) που χωρίζονται από μία απόσταση ~ 5.1 Å. Ακόμα, διαμοριακές αντισιδηρομαγνητικές αλληλεπιδράσεις μέσω π-τροχιακών των φαινυλ-δακτυλίων παρατηρήθηκαν για αυτές τις ενώσεις κάτω από τους 8 K. Η σιδηρομαγνητική σύζευξη που παρατηρείται στις εξαπυρηνικές ενώσεις 1·4H₂O και 3·4H₂O συζητείται επίσης στη βάση *ab initio* UHF υπολογισμών σε μία ένωση-μοντέλο. Η τιμή της σταθεράς σύζευξης (3.7 cm⁻¹) για αυτήν την ένωση μοντέλο, που υπολογίστηκε με χρησιμοποίηση της προσέγγισης “σπασμένης” συμμετρίας, βρίσκεται σε καλή συμφωνία τόσο στο πρόσημο όσο και στο μέγεθος με τις πειραματικά ενρισκόμενες J τιμές (6.00 cm⁻¹ για την ένωση 1·4H₂O και 8.54 cm⁻¹ για την ένωση 3·4H₂O).



Scheme 1. Proposed mechanism for the assembly of the hexanuclear compounds **1**·4H₂O–**4**·2H₂O from tetranuclear mixed valence V^{IV/V} species.

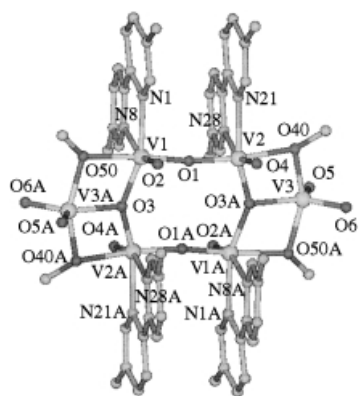


Figure 1. Ball and stick representation of the compound **4**·8CH₃OH and the atom numbering scheme. For clarity the hydrogen atoms are omitted.

the central μ_3 -O3 and μ_3 -O3A oxygen atoms are ligated to the V1, V2A, V3A and V1A, V2, V3 atoms respectively. The six-coordinate V1 and V2 atoms and, by symmetry, the V1A and V2A atoms, are approximately octahedral with the expected distortions associated with the small bite of the 5,5'-me₂bipy rings. The five-coordinate V3 and V3A atoms have distorted trigonal bipyramidal geometry, with V3, O5, O6 and O3A being effectively co-planar. The O40–V3–O50A angle is 151.36 (18)°. The twelve-membered V₆O₆ outer ring is quite planar (mean deviation approximately 0.13 Å) with the

maximum deviation being 0.17 Å for V1 and V1A. The central O3 and O3A atoms are effectively co-planar with the V₆O₆ ring whilst the 5,5'-me₂bipy molecules are close to orthogonal to the V₆O₆ plane. The exocyclic V=O distances are in the range 1.62–1.63 Å. Within the ring the V–O distances are all longer (1.71–2.12 Å), as would be expected. The V1–O1–V2 and V1–O3–V2A angles are 156.7(2) and 146.8(2)°, respectively. The V1–V3A and V2–V3 distances (and, by symmetry, the V1A–V3 and V2A–V3A ones) are about 3.11 Å, while the V1–V2 distance is 3.55 Å.

Alternatively, the cluster can be viewed as a pair of two V₃O₁₃N₄ trimeric units each comprised of two corner-sharing VO₄N₂ octahedra and a VO₅ trigonal bipyramid which has a common edge with each of the VO₄N₂ octahedra. Moreover, the two V₃O₁₃N₄ trimers share two corners represented by two μ_2 -O²⁻ groups.

Bond valence sum (BVS) calculations^[8] as well as the charge requirements suggest that **4**·8CH₃OH is a mixed valence species V₂^{IV}V₄^V. More specifically, the vanadium atoms V1 and V3 exhibit BVS values of 4.94 and 5.11, respectively and thus are clearly identified as V^V centers, while the vanadium atom V2 shows a BVS value of 4.05 and is therefore assigned as a V^{IV} center. The BVS values of the bridged oxo groups μ_2 -O1 and μ_3 -O3 are 1.94 and 2.03, respectively, indicating no protonation for these oxygen atoms. In addition, the BVS values for the methoxy oxygen atoms O40 and O50 are 1.97 and 1.86, respectively, and reveal that they are not protonated. These BVS calculations further confirm that O40 and O50 belong to methoxy groups and not to methyl alcohol ligands.

At this point, it is worth noting that the molecular structures of **1**·2H₂O and **4**·8CH₃OH, which are made up of two (V₃O₁₃N₄) trimeric moieties sharing two corners with the six vanadium centers in a planar cyclic arrangement (Figure 1), are unique among polyoxovanadates and polyoxometalates in general. The majority of known vanadium hexametallates have an approximately O_h symmetry. These V₆ species are considered as derivatives of the hypothetical [V₆VO₁₉]⁸⁻ structure.^[9] Planar V₆ rings have also been reported in the compounds [(V^{IV}O)₆(OH)₉(CO₃)₄]⁵⁻,^[10] and [(V^VO)₆(O)₆(OH)₃(O₂CCH₂CH₂NH₃)₃(SO₄)]⁺,^[11] as well as in the mixed valence V^{IV/V} hexameric cluster [(V^VO)₅(V^{IV}O)(O)₄(PhCO₂)₉].^[12] However, the molecular structures of the

Table 1. Selected interatomic distances and angles relevant to the coordination sphere for the vanadium atoms for compound **4**·8CH₃OH and **1**·2H₂O (square brackets).

bond lengths [Å]					
V1–O1	1.707(4) [1.761(13)]	V1–O3	1.862(3) [1.866(12)]	V1–N1	2.156(4) [2.15(2)]
V1–O2	1.617(3) [1.598(13)]	V1–O50	2.124(4) [2.058(15)]	V1–N8	2.319(4) [2.33(2)]
V2–O1	1.917(4) [1.873(13)]	V2–O40	2.019(4) [2.03(2)]	V2–N21	2.160(5) [2.15(2)]
V2–O4	1.630(4) [1.608(13)]	V2–O3A	1.952(3) [1.916(13)]	V2–N28	2.302(5) [2.33(2)]
V3–O5	1.628(4) [1.621(13)]	V3–O50A	1.962(3) [1.939(14)]	V3–O40	1.977(3) [1.958(14)]
V3–O6	1.625(4) [1.67(2)]	V3–O3A	1.974(4) [2.017(14)]		
bond angles [°]					
V1–O1–V2	156.67(19) [153.6(8)]	V1–O3–V2A	146.8(2) [149.3(8)]		
V1–O3–V3A	108.31(16) [106.3(6)]	O1–V2–N28	79.41(18) [81.5(6)]		
O1–V2–N21	97.22(18) [90.2(6)]	O50A–V3–O40	151.36(18) [147.9(6)]		
O6–V3–O5	107.7(2) [110.7(8)]				

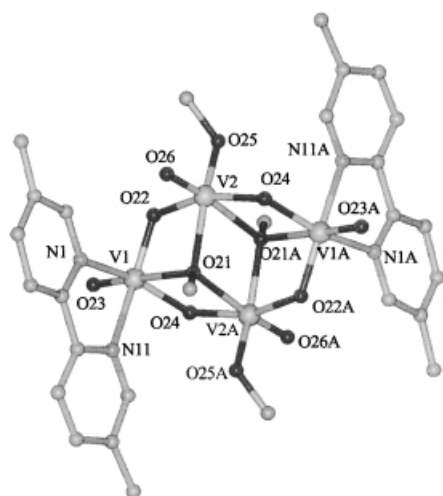
first two compounds consist of six edge-sharing VO₆ octahedra (Anderson-like structure^[3a]) and the structure of the third one is made up of binuclear and tetranuclear units linked together by four benzoate groups.

The molecular structure of compound **5**·3CH₃OH was also identified by X-ray crystal structure analysis. Selected interatomic distances and angles relevant to the coordination sphere of the vanadium atoms for **5**·3CH₃OH are given in Table 2. As is shown in Figure 2, **5**·3CH₃OH consists of a centrosymmetric tetranuclear unit in which the vanadium centers are connected through μ_3 -CH₃O[−] and μ_2 -O^{2−} bridges. The tetramer can be described as a dicubane-like framework with two missing vertices, in which two types of vanadium atoms,

namely V1 and V2, can be distinguished. The crystallographically-related V2 and V2A, which occupy two vertices of the common face of the dicubane unit, are coordinated, in a severely distorted octahedral geometry, by two μ_2 -O^{2−} groups, two μ_3 -CH₃O[−] groups, a terminal CH₃O[−] group and an oxo group. The other two crystallographically related vanadium centers V1 and V1A are also coordinated, in a distorted octahedral geometry, by two 5,5'-me₂bipy nitrogen atoms, two μ_2 -O^{2−} atoms, an oxo group and a μ_3 -CH₃O[−] group. The cluster could also be described as a binuclear unit of edge-sharing VO₆ octahedra, bridged by two VO₄N₂ octahedra each sharing two edges with the binuclear core. Estimation of the oxidation states of the two crystallographically-independent vanadium centers V1 and V2, using BVS calculations^[8], gives a value of 5.00 for each metal atom, which is in agreement with that based on stoichiometry. Furthermore, the doubly bridged oxygen atoms O22 and O24 show BVS values of 1.80, which indicates no protonation for these oxo groups. The BVS values for the methoxy oxygen atoms O21 and O25 are 1.80 and 1.90, respectively, revealing the deprotonation of these oxygen atoms.

Table 2. Selected interatomic distances and angles relevant to the coordination sphere for the vanadium atoms for compound **5**·3CH₃OH.

bond lengths [Å]					
V1–O23	1.598(5)	V1–O24	1.831(4)	V1–N1	2.135(6)
V1–O22	1.734(4)	V1–O21	2.293(4)	V1–N11	2.196(6)
V2–O26	1.601(5)	V2–O24A	1.825(4)	V2–O22	1.982(4)
V2–O25	1.784(5)	V2–O21A	2.326(4)	V2–O21	2.055(4)
bond angles [°]					
V1–O21–V2A	86.36(14)	V2–O21–V2A	105.46(18)		
V1–O22–V2	114.4(2)	V2A–O24–V1	119.6(2)		
N1–V1–O21	84.41(18)	O26–V2–O25	101.7(3)		

Figure 2. Ball and stick representation of the compound **5**·3CH₃OH and the atom numbering scheme. For clarity the hydrogen atoms are omitted.

Infrared spectroscopy: Assignments of some diagnostic bands for compounds **1**·4H₂O–**5**·3CH₃OH are given in Table 3. The infrared spectra of all hexanuclear compounds **1**·4H₂O–**4**·H₂O showed three bands in the frequency range 960–900 cm^{−1} attributable to a V=O stretching vibration, while the IR spectrum of the tetramer **5**·3CH₃OH exhibited only two V=O stretches in the same range. Furthermore, the spectra of the phen-containing species **1**·4H₂O and **2**·6H₂O exhibited a strong band at about 1626 cm^{−1} corresponding to C=C and C=N stretching vibrations, while the respective band in the IR spectra of the bipy-containing species **3**·4H₂O–**5**·3CH₃OH appeared at about 1600 cm^{−1}. Moreover, the absorption bands at 1024–1066 cm^{−1} observed in the IR

Table 3. Diagnostic infrared bands [cm^{−1}] for the compounds **1**·4H₂O–**5**·CH₃OH.

Compound	$\nu(\text{O}-\text{CH}_3)$	$\nu(\text{C}=\text{C}, \text{C}=\text{N})$	$\nu(\text{V}=\text{O})$
1 ·4H ₂ O	1066(s)	1626(s)	950(vs), 925(m), 902(m)
2 ·6H ₂ O	1064(s)	1626(s)	950(vs), 934(m), 907(m)
3 ·4H ₂ O	1062(s), 1024(m)	1600(vs)	951(vs), 930(sh)(w), 915(w)
4 ·H ₂ O	1062(m), 1049(s)	1603(s)	952(vs), 927(m), 902(m)
5 ·CH ₃ OH	1052(s), 1030(m)	1604(m)	957(vs), 941(s)

spectra of all the vanadium compounds $1 \cdot 4\text{H}_2\text{O} - 5 \cdot 3\text{CH}_3\text{OH}$, are attributable to a C–O stretching vibration arising from the coordinated methoxy groups.

UV/Vis solid state reflectance spectroscopy: The hexameric compounds $1 \cdot 4\text{H}_2\text{O} - 4 \cdot \text{H}_2\text{O}$ were not soluble in any common organic solvent or water. We were therefore unable to perform any solution studies. However, the UV/Vis solid state reflectance spectra of $1 \cdot 4\text{H}_2\text{O} - 4 \cdot \text{H}_2\text{O}$ were recorded. The phen-containing species $1 \cdot 4\text{H}_2\text{O}$ and $2 \cdot 6\text{H}_2\text{O}$ exhibited quite similar spectra. These contained a shoulder in the visible region (at 528 nm for $1 \cdot 4\text{H}_2\text{O}$ and 521 nm for $2 \cdot 6\text{H}_2\text{O}$) as well as two peaks in the ultraviolet region (at 269 and 220 nm for $1 \cdot 4\text{H}_2\text{O}$ and 277 and 220 nm for $2 \cdot 6\text{H}_2\text{O}$). The visible spectra of the bipy-containing species $3 \cdot 4\text{H}_2\text{O}$ and $4 \cdot \text{H}_2\text{O}$ exhibited a peak at 495 nm and a shoulder at 498 nm, respectively. In the ultraviolet region, the spectra of $3 \cdot 4\text{H}_2\text{O}$ and $4 \cdot \text{H}_2\text{O}$ revealed three peaks ($\lambda_{\text{max}} = 284, 240$ and 219 nm) and four peaks ($\lambda_{\text{max}} = 315, 290, 249$ and 220 nm), respectively.

Thermogravimetric analysis: The thermal stability of the hexamers $1 \cdot 4\text{H}_2\text{O} - 4 \cdot 6\text{H}_2\text{O}$ under a dinitrogen atmosphere in the range 30–600 °C was examined by TGA-DTA experiments. The total weight loss of $1 \cdot 4\text{H}_2\text{O}$ and $2 \cdot 4\text{H}_2\text{O}$ is 26.3 and 26.5% of their initial weight, respectively. The major weight loss of $1 \cdot 4\text{H}_2\text{O}$ and $2 \cdot 4\text{H}_2\text{O}$ occurred in the range 280–500 °C (13.14%) and 230–415 °C (15.15%), respectively.^[13] The weight losses of $1 \cdot 4\text{H}_2\text{O}$ at 30–130 °C (5.40%) and $2 \cdot 6\text{H}_2\text{O}$ at 30–140 °C (6.48%) are attributed to the release of four (5.09% calculated) and six (7.17% calculated) water molecules per formula unit of $1 \cdot 4\text{H}_2\text{O}$ and $2 \cdot 4\text{H}_2\text{O}$, respectively. On the other hand, the bipy-containing hexamers $3 \cdot 4\text{H}_2\text{O}$ and $4 \cdot \text{H}_2\text{O}$ exhibited a total weight loss of about 49% and 41.6%, respectively. The major weight losses of $3 \cdot 4\text{H}_2\text{O}$ were observed at 220–330 °C (13.28%) and 390–440 °C (12.01%). The major weight losses of $4 \cdot \text{H}_2\text{O}$ were observed at 100–245 °C (17.13%) and 245–390 °C (13.69%). In addition, the weight losses of $3 \cdot 4\text{H}_2\text{O}$ and $4 \cdot \text{H}_2\text{O}$ in the range 30–100 °C (5.36% for $3 \cdot 4\text{H}_2\text{O}$, 0.94% for $4 \cdot \text{H}_2\text{O}$) correspond to the removal of four (5.36% calculated) and one (1.31% calculated) water molecule per formula unit of $3 \cdot 4\text{H}_2\text{O}$ and $4 \cdot 4\text{H}_2\text{O}$, respectively.^[13]

Magnetic study of compounds $1 \cdot 4\text{H}_2\text{O}$ and $3 \cdot 4\text{H}_2\text{O}$: Variable-temperature, solid-state magnetic susceptibility data were collected on powdered samples in a 0.1 T applied magnetic field and in the temperature range 2.0–300 K. The $\chi_{\text{M}}T$ data versus temperature for both hexameric species $1 \cdot 4\text{H}_2\text{O}$ and $3 \cdot 4\text{H}_2\text{O}$ are shown in Figure 3A. The $\chi_{\text{M}}T$ value for compound $1 \cdot 4\text{H}_2\text{O}$ increases from $0.76 \text{ cm}^3 \text{ mol}^{-1} \text{ K}$ at 300 K to $0.90 \text{ cm}^3 \text{ mol}^{-1} \text{ K}$ at 8 K, then drastically decreases to $0.842 \text{ cm}^3 \text{ mol}^{-1} \text{ K}$ at 2 K. The high-temperature value of $0.76 \text{ cm}^3 \text{ mol}^{-1} \text{ K}$ for $\chi_{\text{M}}T$ is very close to the value of $0.75 \text{ cm}^3 \text{ mol}^{-1} \text{ K}$, that is, the spin-only value expected for a $d^1 - d^1$ system with isotropic $g = 2.0$. From the magnetic data it is clear that there are two magnetic ions and therefore complete localization of the single 3d electrons on the two vanadium(IV) ions labeled as V2 and V2A in Scheme 2.

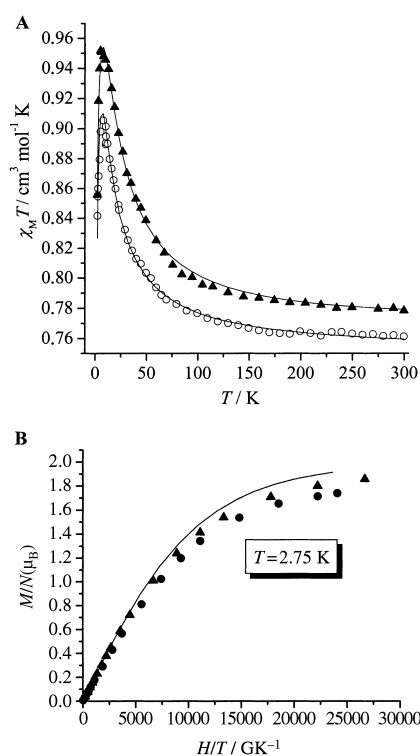
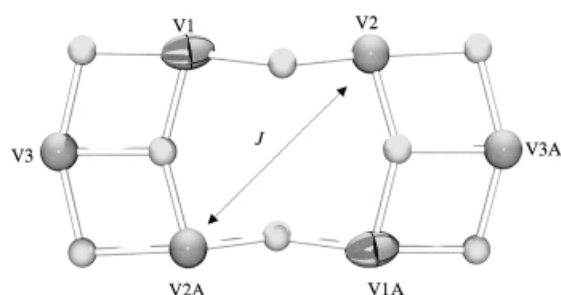


Figure 3. A) Temperature dependence of the susceptibility data, in the form of $\chi_{\text{M}}T$ vs T , for the compounds $1 \cdot 4\text{H}_2\text{O}$ (○) and $3 \cdot 4\text{H}_2\text{O}$ (▲). The solid lines represent the fitting results according to Equation (2); B) magnetization data for the compounds $1 \cdot 4\text{H}_2\text{O}$ (●) and $3 \cdot 4\text{H}_2\text{O}$ (▲). The solid line represents the theoretical Brillouin function for an $S = 1$ system.



Scheme 2. A simplified magnetic model in which the two paramagnetic ions (V2 and V2A) are clearly shown as is the long diamagnetic path between them.

Furthermore the data are consistent with ferromagnetic interaction between the two V^{IV} ions, while below 8 K an antiferromagnetic intermolecular interaction is present due to the strong π -stacking between different hexanuclear clusters (Figure 4). In Figure 4, it can easily be seen that the phenanthroline ring of the V2 atom of one cluster has a π -contact with that of the V2A of the other cluster. The overlap of the two phenanthroline rings is around 80%, while the distance between them is 3.4 \AA . This confirms the strong character of the π -type intermolecular interaction which is irrespective of the large distance between the V^{IV} atoms. Furthermore in this Figure there are two such contacts: a) the phenyl ring of V2 with the phenyl ring of V2A of the upper molecule and b) phenyl ring of V2A with the phenyl ring of V2 of the lower molecule.

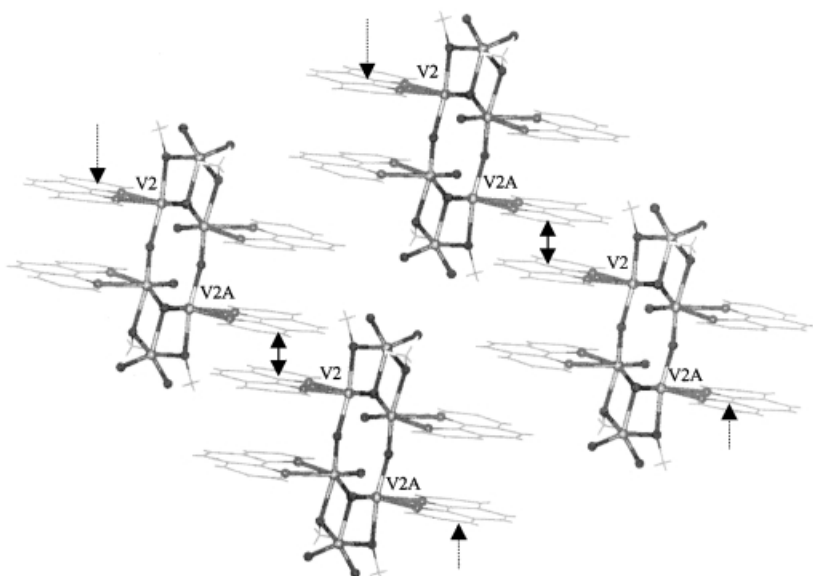


Figure 4. Packing diagram of $1 \cdot 2\text{H}_2\text{O}$. The arrows show the distance (3.4 Å) between the phenanthroline rings of V2 and V2A atoms from two adjacent V6 clusters.

The $\chi_M T$ value for compound $3 \cdot 4\text{H}_2\text{O}$ increases from $0.779 \text{ cm}^3 \text{ mol}^{-1} \text{ K}$ at 300 K to $0.95 \text{ cm}^3 \text{ mol}^{-1} \text{ K}$ at 8 K, then drastically decreases to $0.855 \text{ cm}^3 \text{ mol}^{-1} \text{ K}$ at 2 K. The interaction is again ferromagnetic, while below 8 K the intermolecular interaction seems to be weaker than that of $1 \cdot 4\text{H}_2\text{O}$. The above data were fitted to the Bleaney–Bowers equation based on the mean-field correction, in order to take into account the antiferromagnetic intermolecular interactions. The equation is as follows:

$$\chi_M = \frac{2N g^2 \mu_B^2}{k(T - \theta)} \left(\frac{1}{3 + e^{-\frac{2J}{kT}}} \right) \quad (2)$$

The fitted results are: Compound $1 \cdot 4\text{H}_2\text{O}$: $J = 6.0 \text{ cm}^{-1}$, $g = 2.01$, $\theta = -0.5 \text{ K}$; Compound $3 \cdot 4\text{H}_2\text{O}$: $J = 8.54 \text{ cm}^{-1}$, $g = 2.01$, $\theta = -0.36 \text{ K}$. These are shown as solid lines in Figure 3A.

The magnetization data for both hexameric species are shown in Figure 3B, where the saturation value M_S is close to 1.86 for both compounds. The solid line shows the theoretical Brillouin function for an $S = 1$ system. The small difference between the experimental data and the theoretical curve reflects the significance of the intermolecular interactions, which at this temperature influences the magnetic behaviour of these systems.

EPR Studies for $1 \cdot 4\text{H}_2\text{O}$ and $3 \cdot 4\text{H}_2\text{O}$: In order to confirm the ferromagnetic interaction in these clusters, powder X-band EPR measurements were carried out in the low temperature range (4–70 K) and the spectra at 4 K are shown in Figure 5. For both species, a main resonance was centered at $g = 2.0$, while a resonance centered at $g = 3.9$, corresponding to the half-field transition ($\Delta m_s = \pm 2$), was clearly resolved, which shows the integer character of the ground state. The ratio of intensity between the main resonance and the low-field one was 10:1 for both compounds. Furthermore, the lower intensity of the half-field transition reflects the weak

ferromagnetic interaction between the paramagnetic vanadium(IV) ions. This was also confirmed from the magnetic measurements (see above) and it is in accordance with the large distance between the V^{IV} centers. Temperature dependence experiments in the temperature range 4–70 K showed no significant change of the linewidth, which is further evidence of localized unpaired electrons.

Theoretical calculations: A theoretical study of the hexanuclear compounds has been also carried at the UHF level. The very large size of the compounds makes it very difficult to carry out ab initio calculations. Therefore, with the aim of speeding up the calculations, the theoretical study was undertaken using a model in which the phen and bipy ligands were replaced

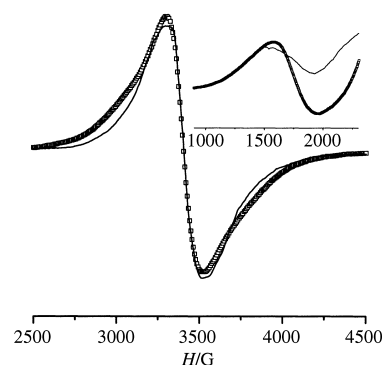


Figure 5. Powder X-band EPR spectra of compounds $1 \cdot 4\text{H}_2\text{O}$ (\square) and $3 \cdot 4\text{H}_2\text{O}$ (—) in the field range 2500–4500 G. The half-field transition for the two hexamers is shown in the inset.

by the model ligand $[\text{HN}=\text{CH}-\text{CH}=\text{NH}]$. This model ligand has the same donor atoms and closely resembles the conjugated system of phen or bipy. Such a model has also been used successfully in other metal compounds containing these ligands.^[14]

The overlay of the optimized structure and the experimental structure for $4 \cdot 8\text{CH}_3\text{OH}$ is shown in Figure 6. Some selected calculated structural parameters are reported in Table 4. In general, taking into account that the model is simplified and doubtless less hindered, one observes quite satisfactory agreement between the model and the experimental values of geometrical parameters of both $1 \cdot 2\text{H}_2\text{O}$ and $4 \cdot 8\text{CH}_3\text{OH}$.

In the optimized structure the expectation value of the spin operator $\langle S^2 \rangle$ was 2.026. The calculated Mulliken atomic spin densities for V1, V2 and V3 were 0.028, 0.904, and 0.014, respectively, whereas those according to Lowdin analysis were 0.031, 0.894, and 0.012, respectively. The results of the spin population analysis further confirm the characterization of V1 and V3 as V^{V} and V2 as V^{IV} , in line with

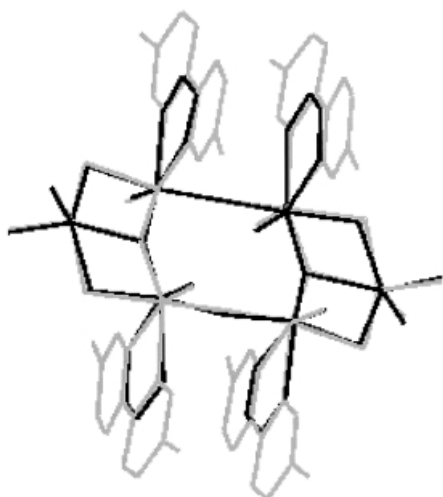


Figure 6. Overlay of the optimized structure of the model complex **1'** in black and the experimental structure of **4·8CH₃OH** in grey (hydrogens not shown).

Table 4. Selected bond lengths [Å] and bond angles [°] calculated for the model complex **1'**.^[a]

	calcd		calcd
V1–O1	1.716	O1–V1–O3	100.5
V1–O2	1.541	O1–V1–N1	90.8
V1–O3	1.849	O3–V1–O50A	77.6
V1–O50A	1.995	O50A–V1–N1	81.3
V1–N1	2.187	O2–V1–N8	158.7
V1–N8	2.392	N1–V1–N8	68.5
V2–O1	1.919	O1–V2–O3A	98.4
V2–O4	1.527	O1–V2–N21	88.1
V2–O3A	1.837	O3A–V2–O40	77.0
V2–O40	1.986	O40–V2–N21	90.2
V2–N21	2.216	O4–V2–N28	164.0
V2–N28	2.374	N21–V2–N28	69.9
V3–O5	1.548	O5–V3–O3A	120.5
V3–O6	1.653	O6–V3–O3A	139.4
V3–O40	1.923	O5–V3–O6	110.1
V3–O50	1.917	O40–V3–O50	142.1
V3–O3A	2.082	V1–O1–V2	158.7
		V1–O3–V2A	150.2
		V2–O40–V3	106.0
		V3–O50–V1A	103.7
		V1–O3–V3A	106.6
		V3–O3A–V2	103.2

[a] Numbering scheme as in Figure 1.

the bond-valence sum calculations, and serve as an indication for the strong localization of each unpaired electron on a vanadium atom. Thus, it is obvious that we are dealing with an essentially d^1-d^1 binuclear system.

According to Hoffmann's model for superexchange interactions in binuclear complexes, the degenerate in-phase and out-of-phase d-orbital combinations of the metal fragments interact with the symmetry-appropriate orbitals of the bridging ligands, resulting in two SOMOs. The energy gap between the two SOMOs, ($\Delta = e_1 - e_2$) is closely related to the absolute magnitude of the antiferromagnetic term, J_{AF} , of the superexchange interaction.^[15] According to the UHF calculations, each of the two SOMOs, Φ^S and Φ^{AS} , the shapes of which are presented in Figure 7, is localized to the d orbitals of the V2 and V2A atoms lying in the plane of the $[V_6O_8]$ framework,

with almost zero participations from atomic orbitals of the intervening bridging atoms. As the calculated difference in energy (Δ) of the SOMOs Φ^S and Φ^{AS} is very small (480 cm^{-1}), the antiferromagnetic term is diminished and the ferromagnetic term becomes dominant. This is exactly the situation experimentally observed.

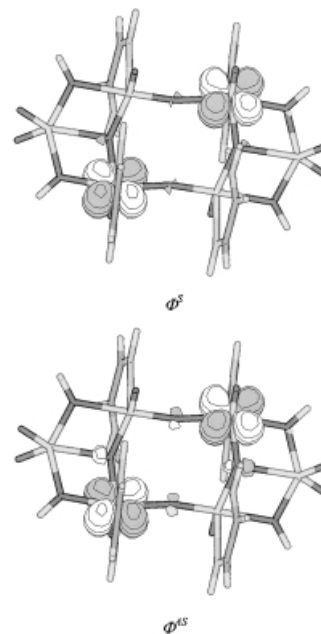


Figure 7. Shapes of the two SOMOs, Φ^S and Φ^{AS} , of the model complex **1'**.

The large size of the system prevents the application of a configuration interaction calculation which, in principle, should be used for the quantitative calculation of the singlet–triplet gap.^[16] Instead, we have used the broken symmetry (BS) approach proposed by Noodleman,^[17, 18] which has been successfully applied to the study of the magnetic properties of binuclear complexes.^[19–22] In this approach the triplet state, $|T\rangle$, is represented approximately by a single spin-unrestricted determinant, because it is a proper pure spin eigenfunction. For the singlet state $|S\rangle$, although a pure spin state should be obtained by a linear combination of the two determinants, $|\alpha\beta\rangle$ and $|\beta\alpha\rangle$, one of these determinants is actually minimized. The energy of this BS solution is related to that of the pure singlet and the singlet–triplet gap can be calculated as:

$$J = 2 \frac{E_{BS} - E_T}{S(S+1)} \quad (3)$$

Using this method we have calculated the exchange coupling constant for this model of the hexanuclear compounds. The calculated value of J (3.7 cm^{-1}) is in agreement in nature and magnitude with the experimental values (6.00 cm^{-1} for **1·4H₂O** and 8.54 cm^{-1} for **3·4H₂O**). The discrepancy is attributed to the neglect of electron correlation at the UHF level, as well as to the effect of modelling.

Conclusion

A series of $V^{IV/V}$ oxo-methoxo-hexametalates $1 \cdot 4H_2O - 4 \cdot H_2O$ was prepared by treating $V^{IV}O^{2+}$ species with an organic nitrogen-donor chelate ligand and triethylamine in methyl alcohol. The tetranuclear dicubane-like compound $5 \cdot 3CH_3OH$ was also isolated from the reaction mixture used for the preparation of $4 \cdot H_2O$. The isolation of this fully oxidized V^V tetranuclear species reveals a possible assembly of the hexanuclear compounds $1 \cdot 4H_2O - 4 \cdot H_2O$ from tetranuclear mixed valence $V^{IV/V}$ units. The crystal structures of $1 \cdot 2H_2O$ and $4 \cdot 8CH_3OH$ revealed a pair of $(V_3O_{13}N_4)$ trimeric units sharing two corners, with the six vanadium centers being in a planar cyclic arrangement. Remarkably, such a structural motif is observed for first time in polyoxometalates.

In marked contrast to the vast majority of known polynuclear vanadium(IV) or (IV/V) species, which exhibit anti-ferromagnetic coupling between $V^{IV}O^{2+}$ magnetic ions, the hexameric compounds $1 \cdot 4H_2O$ and $3 \cdot 4H_2O$ show ferromagnetic behavior. More interestingly, the EPR and magnetic measurements for the species $1 \cdot 4H_2O$ and $3 \cdot 4H_2O$ revealed a complete localization of single 3d electrons on two V^{IV} ions, which surprisingly interact ferromagnetically through a long diamagnetic path of about 5.1 Å. Another interesting feature of the system is the intermolecular antiferromagnetic interactions through π -contacts of phenyl rings observed at temperatures below 8 K. Theoretical UHF calculations have been used to interpret the experimental magnetic data. Both the shape and the energy difference of the two SOMOs calculated for a simplified model of the hexanuclear compounds account well for the observed intramolecular ferromagnetic interaction, while the calculated J value (3.7 cm^{-1}) is in good agreement both in sign and magnitude with the experimental values.

The results obtained herein suggest that other mixed valence $V^{IV/V}$ polyoxo-alkoxo-metalates with appropriate topologies might be a good source of ferromagnetically-coupled systems with large ground state spin values. It is an ongoing challenge for us to expand this class of compounds.

Experimental Section

Materials: Reagent grade chemicals were obtained from Aldrich, and used without further purification. Dichlorobis(tetrahydrofuran)oxovanadium(IV), $[V^{IV}OCl_2(thf)_2]$, was prepared by the literature procedure.^[23] All manipulations were carried out under high-purity argon using standard Schlenk techniques, unless otherwise noted. Methyl alcohol was dried by refluxing over magnesium methoxide, while reagent grade triethylamine was dried and distilled over calcium hydride. C, H, and N analyses were conducted by the University of Ioannina's microanalytical service. Vanadium was determined gravimetrically as vanadium pentoxide or by atomic absorption.

$[V_6O_{12}(\mu_2-OCH_3)_4(phen)_4] \cdot 4H_2O$ ($1 \cdot 4H_2O$): Solid phen (0.290 g, 1.6 mmol) was added in one portion to a stirred solution of $[V^{IV}OCl_2(thf)_2]$ (0.450 g, 1.6 mmol) in methyl alcohol (14 mL). The blue color of the solution immediately changed to green. Triethylamine (0.807 g, 8 mmol) was then added, causing the solution to turn deep red. After stirring for 12 h the solution was left in the atmosphere for two days, during which dark red needle-shaped crystals of $1 \cdot 4H_2O$ were formed. The crystals were filtered off, washed with methyl alcohol (5 mL) and diethyl ether (5 mL), then dried under vacuum to afford $1 \cdot 4H_2O$ (0.184 g, 50%). Elemental analysis

calcd (%) for $C_{52}H_{52}N_8O_{20}V_6$ (1414.63): C 44.15, H 3.70, N 7.92, V 21.60; found C 44.45, H 3.45, N 8.05, V 21.90.

$[V_6O_{12}(\mu_2-OCH_3)_4(5-mephen)_4] \cdot 4H_2O$ ($2 \cdot 6H_2O$): Compound $2 \cdot 6H_2O$ was prepared in 54% yield in a manner similar to $1 \cdot 4H_2O$, using 5-mephen instead of phen. Elemental analysis calcd (%) for $C_{56}H_{68}N_8O_{22}V_6$ (1506.75): C 44.64, H 4.54, N 7.43, V 20.29; found C 44.49, H 4.20, N 7.52, V 20.50.

$[V_6O_{12}(\mu_2-OCH_3)_4(bipy)_4] \cdot 4H_2O$ ($3 \cdot 4H_2O$): Compound $3 \cdot 4H_2O$ was synthesized in 30% yield in an analogous fashion to compound $1 \cdot 4H_2O$, using bipy instead of phen. Elemental analysis calcd (%) for $C_{44}H_{52}N_8O_{20}V_6$ (1318.58): C 40.08, H 3.97, N 8.5, V 23.18; found C 40.22, H 3.85, N 8.58, V 22.85.

$[V_6O_{12}(\mu_2-OCH_3)_4(5,5'-me_2bipy)_4] \cdot H_2O$ ($4 \cdot H_2O$): Compound $4 \cdot H_2O$ was prepared in 44% yield in a fashion similar to $1 \cdot 4H_2O$, using 5,5'-me₂bipy instead of phen. Elemental analysis calcd (%) for $C_{52}H_{70}N_8O_{17}V_6$ (1376.76): C 45.36, H 5.12, N 8.14, V 22.20; found C 45.15, H 5.25, N 8.45, V 22.40.

$[V_4O_8(OCH_3)_2(\mu_3-OCH_3)_2(5,5'-mebipy)_2] \cdot 3CH_3OH$ ($5 \cdot 3CH_3OH$): Compound $5 \cdot 3CH_3OH$ was isolated from the reaction mixture used for the synthesis of $4 \cdot H_2O$. Specifically, yellow crystals of $5 \cdot 3CH_3OH$ were co-precipitated with crystals of $4 \cdot H_2O$ by allowing the final solution to stand at -10°C for eight weeks. The desired crystals were then manually separated from the dark red crystals of $4 \cdot H_2O$. A reproducible route to this material has not yet been determined.

X-ray crystallography: Diffraction measurements for $1 \cdot 2H_2O$, $4 \cdot 8CH_3OH$ and $5 \cdot 3CH_3OH$ were performed on a Siemens SMART diffractometer using a graphite monochromated Mo K radiation. A crystal of $1 \cdot 2H_2O$, $4 \cdot 8CH_3OH$ or $5 \cdot 3CH_3OH$ was sealed in a glass capillary with the mother liquor to avoid decomposition. The crystals of $1 \cdot 2H_2O$ and $4 \cdot 8CH_3OH$ were of poor quality. Crystal data and details of data collection are listed in Table 5. For structure solution and refinement, the programs SHELXS-86^[24] and SHELXS-93^[25] were used. All non-hydrogen atoms for the three structures were refined anisotropically. CCDC-189160 ($1 \cdot 2H_2O$), CCDC-189159 ($4 \cdot 8CH_3OH$) and CCDC-189158 ($5 \cdot 3CH_3OH$) contain the supplementary crystallographic data for this paper. These data can be obtained free of charge at www.ccdc.cam.ac.uk/conts/retrieving.html (or from the Cambridge Crystallographic Data Centre, 12 Union Road, Cambridge CB2 1EZ, UK; fax: (+44) 1223-336033; or deposit@ccdc.cam.ac.uk).

Table 5. Summary of crystallographic data for compounds $1 \cdot 2H_2O$, $4 \cdot 8CH_3OH$, $5 \cdot 3CH_3OH$.^[a]

	$1 \cdot 2H_2O$	$4 \cdot 8CH_3OH$	$5 \cdot 3CH_3OH$
formula	$C_{52}H_{48}N_8O_{18}V_6$	$C_{60}H_{92}N_8O_{24}V_6$	$C_{31}H_{48}N_4O_{15}V_4$
M_r	1378.62	1615.06	922.51
a [Å]	9.717(3)	15.3564(19)	12.507(2)
b [Å]	11.694(4)	17.515(2)	15.066(3)
c [Å]	13.344(5)	14.8273(19)	12.203(2)
α [°]	74.342(6)	90	90
β [°]	77.504(7)	115.586(3)	114.368(4)
γ [°]	88.537(8)	90	90
V [Å ³]	1424.6(8)	3597.0(8)	2094.5(7)
Z	1	2	2
ρ_{calcd} [Mg m ⁻³]	1.607	1.491	1.463
space group	$P\bar{1}$	$P2(1)/c$	$P2(1)/c$
T [K]	293(2) ^[a]	125(2)	293(2)
λ [Å]	0.71073	0.71073	0.71073
μ [mm ⁻¹]	1.023	0.828	0.931
GOF on F^2	0.975	1.020	0.976
$R1(\text{final})$	0.1511	0.1058	0.0571
$wR2$	0.3580	0.2334	0.1246

[a] The structure of $1 \cdot 2H_2O$ could not be determined at low temperature because of problems with the crystal fracturing on cooling.

Physical measurements: IR spectra of the various compounds dispersed in KBr pellets and in Nujol with CsI windows were recorded on a Perkin-Elmer Spectrum GX FT-IR spectrometer. UV/Vis solid state reflectance spectra of the compounds dispersed in $BaSO_4$ were recorded on a Shimadzu 2401-PC system. Thermogravimetric analysis (TGA/DTA) was

performed with a Shimadzu 449C thermal analyses instrument, at a temperature range of 30–600 °C under dinitrogen atmosphere with a heating rate of 5 °C min⁻¹. Polycrystalline powder EPR spectra were recorded for all the compounds at X-band frequency (9.23 GHz) on a Varian ESR9 spectrometer equipped with a continuous flow 4He cryostat, both at room temperature and at helium temperatures of 4–70 K. The temperature dependence of magnetic susceptibility was measured on polycrystalline powder samples using a Cryogenics S600 SQUID Magnetometer with an applied field of 0.1 T and a temperature range of 2–300 K. Data were corrected for sample holder contribution and diamagnetism of the sample using standard procedures.

Computational details: The electronic structure and geometry of the model studied were computed using UHF theory.^[26] For the vanadium atom the effective core potential (ECP) approximation of Hay and Wadt was used with the electrons described by the ECP being those of 1s, 2s, and 2p shells, while the basis set used was of valence double- ζ quality.^[27] For all other atoms the STO-3G basis set was used.^[28] The calculations involved 58 atoms, 264 basis functions and 612 primitive Gaussian functions. Full geometry optimization was carried out without any symmetry constraint, using tight convergence criteria in both optimization and SCF procedures. All of the calculations were performed using the GAMESS package.^[29]

Acknowledgement

We thank the Thermal Analysis Laboratory for performing the thermogravimetric analyses, and Mrs. Cate Statira for her subtle but nonetheless useful contribution to the linguistic refinement of the text.

- [1] Molecular magnetism related books: a) O. Khan, *Molecular Magnetism*, VCH, Weinheim, Germany, **1993**; b) *Magnetic Molecular Materials*, Vol. 198 (Eds.: D. Gatteschi, O. Khan, J. S. Miller, F. Palacio), NATO Asi Series E, Kluwer Academic, Dordrecht (The Netherlands), **1991**; papers concerning magnetic clusters relevant in biochemistry: c) G. Blondin, J. J. Girerd, *Chem. Rev.* **1990**, *90*, 1359; d) G. Christou, *Acc. Chem. Res.* **1989**, *22*, 328.
- [2] a) J. S. Miller, A. J. Epstein, W. M. Reiff, *Science* **1988**, *240*, 40; b) J. M. Manriquez, G. T. Yee, R. S. Mclean, A. J. Epstein, J. S. Miller, *Science* **1991**, *252*, 1415; c) D. Gatteschi, A. Caneschi, L. Pardi, R. Sessoli, *Science* **1994**, *265*, 1054; d) L. Thomas, F. Liondi, R. Ballou, D. Gatteschi, R. Sessoli, B. Barbara, *Nature* **1996**, *383*, 145; e) R. Sessoli, H. L. Chai, A. R. Schake, S. Wang, J. B. Vincent, K. Folting, D. Gatteschi, G. Christou, D. N. Hendrickson, *J. Am. Chem. Soc.* **1993**, *115*, 1804; f) H. J. Eppley, H. L. Tsai, N. de Vries, G. Christou, D. N. Hendrickson, *J. Am. Chem. Soc.* **1995**, *117*, 301.
- [3] a) M. T. Pope, *Heteropoly and Isopoly Oxometalates*, Springer, New York, **1983**; b) M. T. Pope, A. Müller, *Angew. Chem.* **1991**, *103*, 56; *Angew. Chem. Int. Ed. Engl.* **1991**, *30*, 34; c) *Polyoxometalates: From Platonic Solids to Anti-Retroviral Activity* (Eds.: M. T. Pope, A. Müller), Kluwer, Dordrecht (The Netherlands), **1994**; d) *Polyoxometalate Chemistry: From Topology via Self-Assembly to Applications* (Eds.: M. T. Pope, A. Müller), Kluwer, Dordrecht (The Netherlands), **2001**; e) *Chem. Rev.* **1998**, *98*, 8 (guest editor: C. L. Hill).
- [4] a) J. M. Clemente-Juan, E. Coronado, *Coord. Chem. Rev.* **1999**, *193–195*, 361 and references therein; b) A. Müller, F. Peters, M. T. Pope, D. Gatteschi, *Chem. Rev.* **1998**, *98*, 239 and references therein.
- [5] a) J. S. Miller, A. J. Epstein, *Chem. Commun.* **1998**, 1319; b) J. P. Fitzgerald, B. B. Kaul, G. T. Yee, *Chem. Commun.* **2000**, 49.
- [6] a) S. I. Castro, Z. Sun, J. C. Bollinger, D. N. Hendrickson, G. Christou, *Chem. Commun.* **1995**, 2517; b) Z. Sun, C. M. Grant, S. L. Castro, D. N. Hendrickson, G. Christou, *Chem. Commun.* **1995**, 2517; c) S. L. Castro, Z. Sun, C. M. Grant, J. C. Bollinger, D. N. Hendrickson, G. Christou, *J. Am. Chem. Soc.* **1998**, *120*, 2365; d) D. Grohol, D. Papoutsakis, D. G. Nocera, *Angew. Chem.* **2001**, *113*, 1519; *Angew. Chem. Int. Ed.* **2001**, *40*, 1519.
- [7] a) W. Plass, *Angew. Chem.* **1996**, *108*, 699; *Angew. Chem. Int. Ed. Engl.* **1996**, *35*, 627; b) J. T. Wroblewski, M. R. Thompson, *Inorg. Chim. Acta* **1988**, *150*, 269; c) G. B. Karet, Z. Sun, D. D. Heinrich, J. K. McCusker, K. Folting, W. E. Streib, J. C. Huffman, D. N. Hendrickson, G. Christou, *Inorg. Chem.* **1996**, *35*, 6450; d) T. Ishida, S. Mitsubori, T. Nogami, N. Takeda, M. Ishikawa, H. Iwamura, *Inorg. Chem.* **2001**, *40*, 7059.
- [8] I. D. Brown, in *Structure and Bonding in Crystals, Vol. II* (Eds.: M. O'Keefe, A. Navrotsky), Academic Press, New York, **1981**, p. 1–30.
- [9] a) Q. Chen, D. P. Goshorn, C. P. Scholes, X. Tan, J. Zubieta, *J. Am. Chem. Soc.* **1992**, *114*, 4667; b) M. I. Khan, Q. Chen, H. Höpe, S. Parkin, C. J. O'Connor, J. Zubieta, *Inorg. Chem.* **1993**, *32*, 2929.
- [10] T. C. W. Mak, P.-J. Li, C.-M. Zheng, K.-Y. Huang, *Chem. Commun.* **1986**, 1597.
- [11] C. H. Ng, C. W. Lim, S. G. Teoh, H.-K. Fun, A. Usman, S. W. Ng, *Inorg. Chem.* **2002**, *41*, 2.
- [12] D. Rehder, W. Pribsch, M. V. Oeynhaus, *Angew. Chem.* **1989**, *101*, 1295; *Angew. Chem. Int. Ed. Engl.* **1989**, *28*, 1221.
- [13] According to the X-ray crystallographic analysis, **1**·2H₂O and **4**·8CH₃OH contain two water and eight methyl alcohol lattice molecules, respectively. The difference between the TG and crystallographic data for these compounds concerning the content of their lattice solvent molecules can be explained by taking into account that the crystal data for both compounds were collected on a single crystal in its mother liquor. It seems that the crystals of **1**·2H₂O, outside their mother liquor, absorb two more water molecules and thus, the TG analysis shows four water molecules per formula unit of **1**·4H₂O rather than the two lattice H₂O molecules found by X-ray crystallography. On the other hand, it seems that the crystals of **4**·8CH₃OH, outside their mother liquor, lose their methyl alcohol content and simultaneously, they absorb one water molecule.
- [14] E. J. Tolis, M. J. Manos, A. J. Tasiopoulos, C. P. Raptopoulou, A. Terzis, M. P. Sigalas, Y. Deligiannakis, T. A. Kabanos, *Angew. Chem.* **2002**, *114*, 2921; *Angew. Chem. Int. Ed.* **2002**, *41*, 2797.
- [15] P. J. Hay, J. C. Thibeault, R. Hoffmann, *J. Am. Chem. Soc.* **1975**, *97*, 4884.
- [16] F. Illas, I. D. P. R. Moreira, C. de Graaf, V. Barone, *Theor. Chem. Acc.* **2000**, *104*, 265.
- [17] L. Noodleman, D. A. Case, *Adv. Inorg. Chem.* **1992**, *38*, 423.
- [18] L. Noodleman, C. Y. Peng, D. A. Case, J. M. Mouesda, *Coord. Chem. Rev.* **1995**, *144*, 199.
- [19] E. Ruiz, P. Alemany, S. Alvarez, J. Cano, *J. Am. Chem. Soc.* **1997**, *119*, 1297.
- [20] E. Ruiz, P. Alemany, S. Alvarez, J. Cano, *Inorg. Chem.* **1997**, *36*, 3683.
- [21] J. Cano, P. Alemany, S. Alvarez, E. Ruiz, M. Verdaguier, *Chem. Eur. J.* **1998**, *4*, 476.
- [22] C. López, R. Costa, F. Illas, E. Molins, E. Espinoza, *Inorg. Chem.* **2000**, *39*, 4560.
- [23] R. Kern, *J. Inorg. Nucl. Chem.* **1962**, *24*, 1105.
- [24] G. M. Sheldrick, SHELXS-86: Structure solving program, University of Göttingen (Germany), **1986**.
- [25] G. M. Sheldrick, SHELXS-93: Crystal structure refinement, University of Göttingen (Germany), **1993**.
- [26] J. A. Pople, R. K. Nesbet, *J. Chem. Phys.* **1954**, *22*, 571.
- [27] P. J. Hay, W. R. Wadt, *J. Chem. Phys.* **1985**, *82*, 299.
- [28] W. J. Hehre, R. F. Stewart, J. A. Pople, *J. Chem. Phys.* **1969**, *51*, 2657.
- [29] M. W. Schmidt, K. K. Baldrige, J. A. Boatz, S. T. Elbert, M. S. Gordon, J. J. Jensen, S. Koseki, N. Matsunaga, K. A. Nguyen, S. Su, T. L. Windus, M. Dupuis, J. A. Montgomery, *J. Comput. Chem.* **1993**, *14*, 1347.

Received: July 26, 2002 [F4284]